Northumbria Research Link

University**Library**

RISE-Based Integrated Motion Control of Autonomous Ground Vehicles With Asymptotic Prescribed Performance

Chuan Hu, Hongbo Gao, Jinghua Guo, Hamid Taghavifar, *Member, IEEE*, Yechen Qin, *Member, IEEE*, Jing Na, *Member, IEEE*, and Chongfeng Wei

Abstract—This article investigates the integrated lane-keeping and roll control for autonomous ground vehicles (AGVs) considering the transient performance and system disturbances. The robust integral of the sign of error (RISE) control strategy is proposed to achieve the lane-keeping control purpose with rollover prevention, by guaranteeing the asymptotic stability of the closed-loop system, attenuating systematic disturbances, and maintaining the controlled states within the prescribed performance boundaries. Three contributions have been made in this article: 1) a new prescribed performance function (PPF) that does not require accurate initial errors is proposed to guarantee the tracking errors restricted within the predefined asymptotic boundaries; 2) a modified neural network (NN) estimator which requires fewer adaptively updated parameters is proposed to approximate the unknown vertical dynamics; and 3) the improved RISE control based on PPF is proposed to achieve the integrated control objective, which analytically guarantees both the controller continuity and closed-loop system asymptotic stability by integrating the signum error function. The overall system stability is proved with the Lyapunov function. The controller effectiveness and robustness are finally verified by comparative simulations using two representative driving maneuvers, based on the high-fidelity CarSim–Simulink simulation.

Index Terms—Autonomous ground vehicles (AGVs), lane keeping, neural network (NN), prescribed performance control (PPC), robust integral of the sign of the error (RISE), roll control.

I. INTRODUCTION

RECENT vehicular technologies in both the cyber and physical systems and insistent society demands for the transportation security and efficiency [1]–[3] have greatly accelerated the advancement of autonomous ground vehicles (AGVs) [4], [5]. Complex traffic environment and challenging driving scenarios have brought about higher requirements for AGVs in terms of safety, intelligence, and efficiency [6]–[9]. In this sense, high-performance motion control becomes increasingly important for guaranteeing a safe and robust autonomous driving maneuver [10]. Especially, the integrated vehicle dynamics control in the yaw and roll planes which can further improve the vehicle's overall stability and safety have obtained more research focus and effort [11]–[13].

As the most basic control objective of AGVs, the lane-keeping control is designed to maintain the vehicle to stay on the center line of the desired lane in the presence of inevitable tire sliding effects, system uncertainties, and unknown disturbances [14], [15]. Different lane-keeping control strategies [16]–[21] were proposed previously for various driving scenarios. However, previous literature on the lane keeping or path following control mostly investigated the vehicle dynamics in the yaw plane only, and neglected the roll dynamics or load transfer [19], [22]. Actually, the rollover is a crucial concern for the vehicle design community, which although constitutes only a small proportion of all accidents but constitutes a large proportion of all deaths, as it easily causes severe or fatal injuries. The high fatality rate of the vehicle rollover makes it one of the most dangerous accident types, which whereas was less studied in the autonomous driving control of AGVs. Several vehicle motion control strategies with rollover prevention were proposed for a passenger or heavy vehicles [23]–[25]. However, few related research investigated the roll dynamics control or rollover prevention in the lane-keeping control of AGVs. To the best of our knowledge, there is hardly any literature which combines the lane-keeping control with the vehicle roll dynamics control for AGVs. Integrating multiple dynamics in the motion control of AGVs will complicate the controller design, since more system uncertainties, nonlinearities, disturbances, and dynamics couplings will be involved which may further deteriorate the system stability and transient performance.

Recently, a robust integral of the sign of the error (RISE) control methodology was developed in [26] to compensate for system uncertainties and disturbances. The particular feature of the RISE approach is that it can use the integral of the sign function of the feedback error to assure asymptotic stability. Furthermore, compared with traditional sliding mode control (SMC) approaches, RISE can generate the control continuity, which thus can avoid the chattering effects caused by infinite fast control switching. Very few previous literature had adopted RISE strategy in ground vehicles or autonomous vehicles. In [27], an asymptotically stable controller was proposed for autonomous path following of an unmanned ground vehicle (UGV) using RISE feedback and vector field. In [28], an adaptive feedforward term and a RISE feedback term were combined to yield an asymptotic tracking control for four-wheel steering (4WS) vehicles, which can improve the tracking performance and reduce the control effort. Nevertheless, in previous research on motion control of AGVs, the roll control was not considered, and no literature had considered the transient performance improvement [29] in RISE control, which can further improve the transient tracking performance and robustness. Although RISE control can achieve the asymptotic steady-state convergence, the transient convergence performance is not guaranteed. Especially, when the control input incorporates the online adaptation process, the potential large overshoot and sluggish response may cause implementation difficulties [30].

According to the literature review, it can be found that the lane-keeping control or roll stability control seldom considered the transient performances of the tracking errors, which greatly influence the vehicle safety, mobility efficiency, and ride comfort in practice. Constraining the tracking errors and crucial states in terms of the overshoots and steady-state values can effectively reduce the collision or rollover possibility of AGVs, and improve the trajectory tracking accuracy, vehicle stability, and safety. Recently, a specific state constraint control technique was developed in [31] based on a peculiarly constructed PPF. The developed prescribed performance control (PPC) technique has attracted much attention in the autonomous vehicle system control [32]–[36]. PPC has been increasingly combined with the neural network (NN) [37] to enhance the performance and robustness in the presence of uncertainties or disturbances [38], [39]. It can asymptotically converge the tracking errors to zero and restricted them within the PPF boundaries, which can potentially be utilized in the motion control of AGVs to enhance the tracking performance and safety.

However, the PPF-based control approaches are likely to encounter singularity problems as the controlled variables may pass through the prescribed boundaries. Furthermore, the steady-state error of conventional PPC may only be maintained in a small but nonzero bound, while it is hard to guarantee the property of the asymptotic convergence [32], [40]. In addition, the previous literature on PPC control usually needs the exact information of the initial conditions of the controlled states [31]–[35], [38], which are explicitly incorporated in the nominal performance function. Whereas, the exact initial conditions may be hard to obtain for motion control of

AGVs, that is, some important states, such as the roll angle or sideslip angle are hard to measure, or the initial values of the controlled states may have large measurement errors due to the unknown sensor noise, draft, or inaccuracies in the sensor's initialization phase. That can deteriorate the control performance or even affect the system stability. Therefore, how to concurrently tackle those restrictions and problems needs further investigations.

To this end, this article has proposed a PPF-based RISE control to achieve transient performance improvement and asymptotic steady-state convergence simultaneously. To the best of our knowledge, it is the first time that PPF-based control is adopted in the motion control of AGVs to enhance the path-tracking performance, considering the vehicle lateral, yaw and vertical dynamics simultaneously. Moreover, the proposed PPF control can remedy the stringent requirement on the initial conditions and achieve asymptotic convergence in comparison to the standard PPF methods. The contributions and features of this article can be summarized into the following three aspects.

1) A new PPF is proposed to transform the tracking errors and controlled states without the information of the exact initial values, and then constrain them within the prescribed asymptotic bounds. Compared with the traditional PPC control, the proposed approach has avoided the requirement on the initial condition in the nominal PPF design, which then can effectively make the controller more practical robust and insensitive to uncertain or unknown initial conditions.

2) A modified radial basis function (RBF) NN approach is proposed to approximate the system disturbance, with fewer adaptive parameters to be updated online. Compared with the multilayer NN approach, this single parameter adaptive estimator can make the number of online adaptive parameters drop to only one for each single control input, considerably reducing the computational cost and simplifying the adaptation law design.

3) The PPF and NN are incorporated into the RISE control design, which enables the tracking errors to be constrained in prescribed boundaries and converged to zero asymptotically in the steady state. This feature improves the standard PPF control designs, where the tracking error only converges to a prescribed performance set in steady state, and also improves the transient performance of the standard RISE control scheme by enabling the transient performance to be prescribed.

The asymptotic convergence of the closed-loop system using the proposed controller is proved with the Lyapunov approach, while the transient performance can be prescribed and strictly guaranteed even in the presence of unknown disturbances. The effectiveness of the proposed controller has been verified through high-fidelity comparative simulations on the CarSim platform.

The rest of this article is organized as follows. The lane-keeping kinematics, vehicle lateral, and roll dynamics are modeled in Section II. The main theoretical results about the PPF and NN-based RISE control design for the integral lane
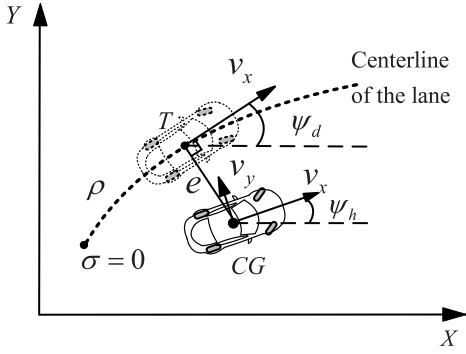
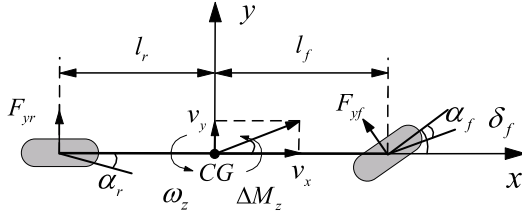Fig. 1.   Vehicle lane-keeping kinematics model.

Fig. 2.   2-DoF model of the vehicle in the presence of sliding effects.

keeping and roll control in Section III. The comparative simulations with a high-fidelity SUV model with CarSim–Simulink are implemented in Section IV. Followed is the conclusion in Section V.

II. PROBLEM FORMULATION

The lane-keeping kinematics model of AGVs can be described by Fig. 1. The lateral offset e is defined as the closest distance from the center of gravity (CG) to the desirable trajectory. The heading error ψ represents the error between the real heading ψ_h and reference heading ψ_d, that is, $\psi = \psi_h - \psi_d$. v_x, v_y, β, and ω_z are the longitudinal velocity, lateral velocity, sideslip angle, and yaw rate, respectively. σ refers to the curvilinear coordinate of the point of tangency T from a predefined point. The curvature of the desirable path is defined as $\rho(\sigma)$ as it changes with the curvilinear coordinate σ. The heading error can usually be assumed small in the lane-keeping maneuver, then its kinematics can be described by

$$\dot{e} = v_x\psi + v_y, \quad \dot{\psi} = \omega_z - \rho(\sigma)v_x. \tag{1}$$

The lane-keeping control objective represents maintaining the vehicle to follow the predefined path asymptotically, that is, to employing an suitable control approach to asymptotically and globally stabilize the lane-keeping errors to zero.

In this article, a 2-degree of freedom (DoF) "bicycle" model [41] is adopted to describe the vehicle dynamics in the yaw plane as shown in Fig. 2. m and I_z represent the total vehicle mass and inertia moment about the yaw axis through the CG, respectively. l_f and l_r represent the distance from the front and rear axles to the CG, respectively. F_{xi} and F_{yi} ($i = 1, 2, 3, 4 = fl, fr, rl, rr$) represent the longitudinal and lateral tire force of the ith tire, respectively. To simplify the controller design, F_{yf} and F_{yr} ($F_{yf} = F_{yfl} + F_{yfr}$ and
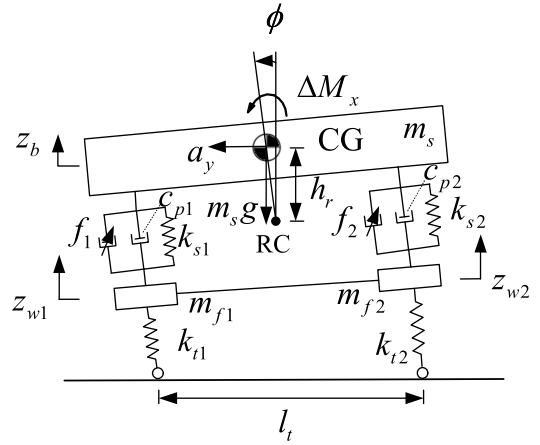
Fig. 3.   Half-car roll dynamics model.

$F_{yr} = F_{yrl} + F_{yrr}$) are used to denote the generalized lateral tire forces of the front and rear tire, respectively. δ_f is the front steering angle. It is assumed that v_x can be maintained constant. The vehicle lateral and yaw dynamics can be modeled as

$$\dot{v}_y = \left(-v_x - \frac{l_f c_f - l_r c_r}{mv_x}\right)\omega_z - \frac{(c_f + c_r)}{mv_x}v_y + \frac{c_f}{m}\delta_f$$

$$\dot{\omega}_z = \frac{(-l_f^2 c_f - l_r^2 c_r)}{v_x I_z}\omega_z + \frac{(l_r c_r - l_f c_f)}{I_z v_x}v_y + \frac{l_f c_f}{I_z}\delta_f + \frac{\Delta M_z}{I_z} \tag{2}$$

where c_f and c_r represent the generalized cornering stiffnesses of the front and rear tires, respectively. ΔM_z is the external yaw moment calculated by

$$\Delta M_z = \sum_{i=1}^{2} F_{xi}\left[(-1)^i\frac{l_t}{2}\cos\delta_f + l_f\sin\delta_f\right] + \sum_{i=3}^{4}(-1)^i\frac{l_t}{2}F_{xi} \tag{3}$$

where l_t is the wheel track. From (1) and (2), the dynamics of the lane-keeping errors can be obtained by canceling the items v_y and ω_z as

$$\ddot{e} = \frac{(c_f + c_r)}{m}\psi - \frac{(c_f + c_r)}{mv_x}\dot{e} - \frac{(l_f c_f - l_r c_r)}{mv_x}\dot{\psi}$$

$$+ \frac{c_f}{m}\delta_f + \left(-v_x^2 - \frac{l_f c_f - l_r c_r}{m}\right)\rho$$

$$\ddot{\psi} = \frac{(l_f c_f - l_r c_r)}{I_z}\psi + \frac{(l_r c_r - l_f c_f)}{I_z v_x}\dot{e} - \frac{(l_f^2 c_f + l_r^2 c_r)}{v_x I_z}\dot{\psi}$$

$$+ \frac{l_f c_f}{I_z}\delta_f + \frac{1}{I_z}\Delta M_z - \frac{(l_f^2 c_f + l_r^2 c_r)}{I_z}\rho \tag{4}$$

by which the requirement of using the information of the lateral velocity is removed, as that is generally hard to measure with low-cost sensors in real applications.

A 4-DoF half-car model [41]–[43] is adopted to model the roll dynamics shown in Fig. 3. The Macpherson strut suspension is adopted in this article. The reasons is that the Macpherson strut can be preassembled into a unit, whose assembly is straightforward. It has a greater width in the

engine compartment through eliminating the upper control arm, which makes Macpherson strut the most widely applied suspension structure [44], [45]. m_s represents the vehicle sprung mass. k_{s1}/k_{s2} represents the left/right side suspension stiffness, c_{p1}/c_{p2} represents the left/right side suspension damping coefficient, m_{f1}/m_{f2} is the left/right unsprung mass of the vehicle, and k_{t1}/k_{t2} is the left/right tire suspension stiffness. z_b and z_{w1}/z_{w2} represent the vertical translations of the sprung mass and left/right unsprung masses. f_1/f_2 is the active force at the front/rear active suspension. ϕ represents the roll angle of the sprung mass. In this article, it is assumed that the vertical translations are not known. The roll dynamics of the sprung mass can be formulated as

$$\left(I_x + m_s h_r^2\right)\ddot{\phi} = m_s h_r\left(a_y \cos\phi + g\sin\phi\right) - \frac{l_t}{2}(F_{s1} - F_{s2}) \tag{5}$$

where I_x is inertia moment along the x-axis. h_r is the distance between the CG of the sprung mass and the roll center. a_y is the lateral acceleration. F_{s1}/F_{s2} is the left/right side dynamics suspension force, and $F_{si}(i = 1, 2)$ can be expressed as

$$F_{si} = -k_{si}\left(z_b - z_{wi} + (-1)^i \frac{l_t \sin\phi}{2}\right)$$
$$- c_{pi}\left(\dot{z}_b - \dot{z}_{wi} + (-1)^i \frac{l_t \dot{\phi}\cos\phi}{2}\right) + f_i. \tag{6}$$

Denote $\Delta M_x = l_t(f_1 - f_2)/2$ as the external roll moment generated by the active suspension. The lateral acceleration is $a_y = \dot{v}_y + v_x\omega_z$, according to which we have

$$\ddot{\phi} = \frac{m_s h_r\left(c_f + c_r\right)}{m\left(I_x + m_s h_r^2\right)}\psi + \frac{\left(m_s h_r g - k_s l_t^2/2\right)}{\left(I_x + m_s h_r^2\right)}\phi$$
$$- \frac{m_s h_r\left(c_f + c_r\right)}{mv_x\left(I_x + m_s h_r^2\right)}\dot{e} - \frac{m_s h_r\left(l_f c_f - l_r c_r\right)}{mv_x\left(I_x + m_s h_r^2\right)}\dot{\psi}$$
$$- \frac{c_p l_t^2}{2\left(I_x + m_s h_r^2\right)}\dot{\phi} + m_s h_r \frac{c_f}{m\left(I_x + m_s h_r^2\right)}\delta_f$$
$$- \frac{1}{\left(I_x + m_s h_r^2\right)}\Delta M_x - \frac{k_s l_t(z_{w1} - z_{w2})}{2\left(I_x + m_s h_r^2\right)}$$
$$- \frac{c_p l_t(\dot{z}_{w1} - \dot{z}_{w2})}{2\left(I_x + m_s h_r^2\right)} - \frac{m_s h_r\left(l_f c_f - l_r c_r\right)}{m\left(I_x + m_s h_r^2\right)}\rho. \tag{7}$$

Considering the lane keeping and roll dynamics simultaneously, the control system can be organized as

$$\dot{x} = Ax + Bu + Ed \tag{8}$$

where $x = [e \ \ \psi \ \ \phi \ \ \dot{e} \ \ \dot{\psi} \ \ \dot{\phi}]^T$ is the system state vector, $u = [u_1 \ u_2 \ u_3]^T$ is the control input with $u_1 = \delta_f$, $u_2 = \Delta M_z$, $u_3 = \Delta M_x$. The vector $d = [\rho \ \ z_{w1} - z_{w2} \ \ \dot{z}_{w1} - \dot{z}_{w2}]^T$ is assumed as a disturbance with unknown bound. The system matrices are expressed as

$$A = \begin{bmatrix} \mathbf{0}_{3\times3} & I_{3\times3} \\ A_{21} & A_{22} \end{bmatrix}, \ B = \begin{bmatrix} \mathbf{0}_{3\times3} \\ B_2 \end{bmatrix}, \ E = \begin{bmatrix} \mathbf{0}_{3\times3} \\ E_2 \end{bmatrix}$$

$$A_{21} = \begin{bmatrix} 0 & a_{42} & 0 \\ 0 & a_{52} & 0 \\ 0 & a_{62} & a_{63} \end{bmatrix}, \ A_{22} = \begin{bmatrix} a_{44} & a_{45} & 0 \\ a_{54} & a_{55} & 0 \\ a_{64} & a_{65} & a_{66} \end{bmatrix}$$

$$B_2 = \begin{bmatrix} b_{41} & 0 & 0 \\ b_{51} & b_{52} & 0 \\ b_{61} & 0 & b_{63} \end{bmatrix}, \ E_2 = \begin{bmatrix} e_{41} & 0 & 0 \\ e_{51} & 0 & 0 \\ e_{61} & e_{62} & e_{63} \end{bmatrix}$$

where

$$a_{42} = \frac{\left(c_f + c_r\right)}{m}, \ a_{44} = -\frac{\left(c_f + c_r\right)}{mv_x}, \ a_{45} = -\frac{\left(l_f c_f - l_r c_r\right)}{mv_x}$$

$$a_{52} = \frac{\left(l_f c_f - l_r c_r\right)}{I_z}, \ a_{54} = \frac{\left(l_r c_r - l_f c_f\right)}{I_z v_x}$$

$$a_{55} = -\frac{\left(l_f^2 c_f + l_r^2 c_r\right)}{v_x I_z}$$

$$a_{62} = \frac{m_s h_r\left(c_f + c_r\right)}{m\left(I_x + m_s h_r^2\right)}, a_{63} = \frac{\left(m_s h_r g - k_s l_t^2/2\right)}{\left(I_x + m_s h_r^2\right)}$$

$$a_{64} = \frac{-m_s h_r\left(c_f + c_r\right)}{mv_x\left(I_x + m_s h_r^2\right)}$$

$$a_{65} = \frac{-m_s h_r\left(l_f c_f - l_r c_r\right)}{mv_x\left(I_x + m_s h_r^2\right)}, \ a_{66} = -\frac{c_p l_t^2}{2\left(I_x + m_s h_r^2\right)}, b_{41} = \frac{c_f}{m}$$

$$b_{51} = \frac{l_f c_f}{I_z}, \ b_{52} = \frac{1}{I_z}, b_{61} = \frac{m_s h_r c_f}{m\left(I_x + m_s h_r^2\right)}$$

$$b_{63} = -\frac{1}{\left(I_x + m_s h_r^2\right)}$$

$$e_{41} = -v_x^2 - \frac{l_f c_f - l_r c_r}{m}, \ e_{51} = -\frac{\left(l_f^2 c_f + l_r^2 c_r\right)}{I_z}$$

$$e_{61} = \frac{m_s h_r\left(l_r c_r - l_f c_f\right)}{m\left(I_x + m_s h_r^2\right)}, e_{62} = -\frac{k_s l_t}{2\left(I_x + m_s h_r^2\right)}$$

$$e_{63} = -\frac{c_p l_t}{2\left(I_x + m_s h_r^2\right)}.$$

Denote $\varepsilon = [\varepsilon_1 \ \ \varepsilon_2]^T$, where $\varepsilon_1 = [x_1 \ \ x_2 \ \ x_3]^T$ and $\varepsilon_2 = [x_4 \ \ x_5 \ \ x_6]^T$, then the control plant (8) can be rewritten as

$$\begin{cases} \dot{\varepsilon}_1 = \varepsilon_2 \\ \dot{\varepsilon}_2 = A_{21}\varepsilon_1 + A_{22}\varepsilon_2 + B_2 u + E_2 d. \end{cases} \tag{9}$$

Remark 1: Note that generally, the vehicle will not roll over without first entering the nonlinear working region. However, as the active suspensions have been applied in this article, we can directly control the roll angle and roll rate, which will then further reduce the rollover possibility. Therefore, the using of linear models should be reasonable, since we did not consider to achieve the "rollover prevention" only until the vehicle has deviated from the linear working region. Actually, we have directly stabilized the roller angle and roll rate to zero for the entire control process, even when the vehicle works in the linear region, which is more strict than the mere rollover prevention. In other words, the proposed control strategy has stabilized the path-following errors and the roll angle to zero [then the vehicle states are bounded according to (1)], which prevents the vehicle from entering the nonlinear region. This control strategy has been widely applied in previous research [46], [47].

The control objective is to design an appropriate controller to ensure that the controlled states (lane-keeping errors and roll angle) can be converged to zero asymptotically, and simultaneously remain in the prescribed performance bounds, considering the disturbance with unknown bound.
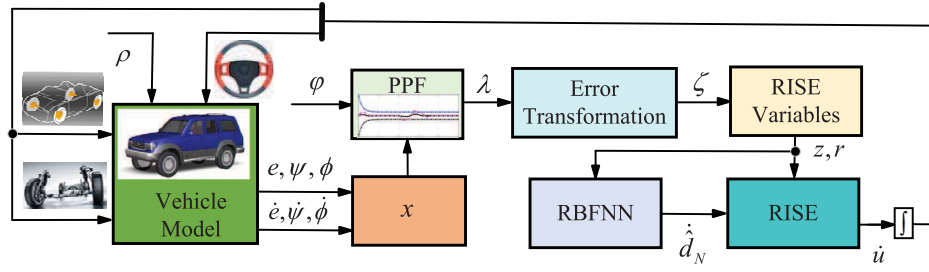
This article has been accepted for inclusion in a future issue of this journal. Content is final as presented, with the exception of pagination.

HU *et al.*: RISE-BASED INTEGRATED MOTION CONTROL OF AGVs WITH ASYMPTOTIC PRESCRIBED PERFORMANCE 5

Fig. 4. Diagram for the closed-loop flow of the proposed PPF-based RISE controller.

III. MAIN RESULTS

This section presents the integrated lane keeping and roll control design that realizes the control objectives described in Section II. First, a modified PPF is constructed to guarantee that the tracking errors are constrained in the predefined regions, where the traditional restriction previously applied on the initial tracking errors is removed. Second, the simplified NN is proposed with only one adaptive law required to approximate the lumped unknown function, which effectively reduce the approximation computation burden. Then the PPF and simplified NN-based RISE control strategy is proposed to realize that the tracking control errors and controlled state are not only maintained within the PPF bound in the transient response but also converged to zero in finite time. The diagram for the closed-loop flow of the proposed PPF-based RISE controller is shown in Fig. 4.

Remark 2: The motivation of using the RISE control is that it can guarantee the asymptotic stability of the closed-loop system, attenuate systematic uncertainties, unmodeled or unknown disturbances, enhance the transient tracking capability, and decrease the steady-state error. Furthermore, the RISE approach can yield continuous control inputs analytically by integrating the signum error function without utilizing the saturation function, which can effectively avoid the chattering effect in traditional SMC. For the motion control of the AGVs, there are unavoidable system uncertainties, external disturbance, and a robust controller that can handle uncertainties and disturbance is desirable in the vehicle motion control. In this context, the RISE controller has significant advantages compared with SMC and is suited for the autonomous driving control.

Remark 3: Indeed, there are worst situations that the prescribed performance cannot handle, such as approaching a sharp turning at a very high speed on a slippery road. However, it should be noted that we focus on general and normal driving maneuvers. In practice, drivers (the same case for the autonomous vehicles) normally will not make sharp turning at very high speeds or on slippery roads. In the simulation cases, we have also chosen two representative driving scenarios, J-turn with a low speed on a slippery road, and lane change with high speed on a dry road. Even if those hazardous situations happen, the vehicle should have already lost stability and control, and any control strategy is hard to stabilize the vehicle.

To this end, before we continue to present the proposed controller design, an assumption should be made to guarantee the feasibility of the proposed control strategy.

Assumption 1: The vehicle drives with normal and safe manoeuvers according to the road conditions (e.g., driving with low speed on slippery roads and steering moderately in high ways), and the vehicle states maintain in the ROA (i.e., the vehicle does not lose stability or control) when the proposed control strategy is applied to implement the path-following and roll control.

A. Prescribed Tracking Performance Function Definition

To reduce the possibility of collisions or rollover, we design the lane-keeping errors and roll angle to satisfy the following prescribed performance:

$$ - \underline{\delta}_i \varphi(t) < x_i < \bar{\delta}_i \varphi(t) \ \forall \ t \geq 0, \ (i = 1, \ 2, \ 3) \tag{10} $$

where $\underline{\delta}_i$ and $\bar{\delta}_i$ are positive constants, and it is usually designed that $\bar{\delta}_i = \underline{\delta}_i$. Equation (10) has determined both the transient and steady-state performance of the controlled state x_i. $\varphi(t)$ is a bounded and smooth function $R^+ \rightarrow R^+$, and called as performance function if $\varphi(t)$ is a strictly decreasing and positive function. Assume $\lim_{t \rightarrow +\infty} \varphi(t) = \varphi_\infty > 0$, where φ_∞ denotes the allowable error in the steady state. To cancel the requirement for the exact initial error, the following modified PPF is chosen as:

$$ \varphi(t) = \coth(vt + \iota) - 1 + \varphi_\infty \tag{11} $$

where v and ι are positive regulating parameters. It is obvious that $\varphi(t)$ satisfies: 1) $\varphi(0) = \coth(\iota) - 1 + \varphi_\infty = (e^{2\iota} + 1)/(e^{2\iota} - 1) - 1 + \varphi_\infty > \varphi_\infty$, where $\varphi(0)$ represents the initial value of $\varphi(t)$ and is denoted as φ_0 for simplicity and 2) $\lim_{\iota \rightarrow 0} \varphi(0) \rightarrow +\infty$, where the limit here is with respect to ι, not the time, with $\iota > 0$ appropriately chosen. By choosing the small ι and positive $\underline{\delta}_i$, $\bar{\delta}_i$, it gets that $\bar{\delta}_i \varphi(0) \rightarrow +\infty$ and $-\underline{\delta}_i \varphi(0) \rightarrow -\infty$. Then the following inequality always holds:

$$ - \underline{\delta}_i \varphi(0) < x_i(0) < \bar{\delta}_i \varphi(0). \tag{12} $$

For general physical systems, inequality (12) should hold, as $x_i(0)$ should be always bounded, and given a sufficiently small l, we have $\lim_{\iota \rightarrow 0} \varphi(0) \rightarrow +\infty$, so that inequality (12) is reasonable. Therefore, the PPF (11) can ensure that (12) is satisfied.

Since the function $\varphi(t)$ is bounded and exponentially decreasing, both the steady-state regulation and transient performance bound of the controlled states x_i can be prescribed *a priori* by selecting appropriate parameters $-\underline{\delta}_i$, $\bar{\delta}_i$, v, ι, φ_0, and φ_∞ that influence the maximum overshoots and the steady-state error bounds. Especially, $-\underline{\delta}_i \varphi(0)$ represents the

This article has been accepted for inclusion in a future issue of this journal. Content is final as presented, with the exception of pagination.

6

IEEE TRANSACTIONS ON SYSTEMS, MAN, AND CYBERNETICS: SYSTEMS

lower boundary of the system transient undershoot, while $\bar{\delta}_i \varphi(0)$ represents the upper boundary of the system transient overshoot. To guarantee the performance constraints are always satisfied, the following transformation is developed:

$$x_i = \varphi(t)S(\zeta_i), \quad (i = 1, \ 2, \ 3) \tag{13}$$

where ζ_i is defined as the transformed error, $S(\zeta_i)$ is a strictly increasing and smooth function chosen as

$$S(\zeta_i) = \frac{\bar{\delta}_i e^{\zeta_i} - \underline{\delta}_i e^{-\zeta_i}}{e^{\zeta_i} + e^{-\zeta_i}}. \tag{14}$$

We can verify that the chosen $S(\zeta_i)$ has the following properties: 1) $-\underline{\delta}_i < S(\zeta_i) < \bar{\delta}_i \ \forall \zeta_i \in L_\infty$ (the vector space L_∞ is a sequence space whose elements are the bounded sequences); 2) $\lim_{\zeta_i \to +\infty} S(\zeta_i) = \bar{\delta}_i$; $\lim_{\zeta_i \to -\infty} S(\zeta_i) = -\underline{\delta}_i$; and 3) $S(\zeta_i)$ is smooth and strictly increasing, and $S(0) = 0$, as it is designed that $\bar{\delta}_i = \underline{\delta}_i$. Moreover, as $\varphi(t) > 0$ we have

$$- \underline{\delta}_i\varphi(t) < \varphi(t)S(\zeta_i) < \bar{\delta}_i\varphi(t). \tag{15}$$

Below, we will employ a lemma to guarantee the proposed PPF constraints can be always satisfied, which is shown as follows.

Lemma 1 [31], [33]: Consider the tracking errors x_i $(i = 1, \ 2, \ 3)$ and the transformed errors ζ_i. If the transformed error ζ_i is bounded and the initial value of the controlled state $x_i(0)$ is always within the performance bounds, i.e., $-\underline{\delta}_i\varphi(0) < x_i(0) < \bar{\delta}_i\varphi(0)$, then x_i will always be maintained in the PPF constraints (10) for all $t \geq 0$.

As $\varphi(t) \neq 0$ we can get the transformed error ζ_i from (14)

$$\zeta_i = S^{-1}(\lambda_i) = \frac{1}{2}\ln\left(\frac{\lambda_i + \underline{\delta}_i}{\bar{\delta}_i - \lambda_i}\right) \tag{16}$$

where $\lambda_i = x_i/\varphi$ represents the intermediate variable. Define $\zeta = [\zeta_1 \ \zeta_2 \ \zeta_3]^{\mathrm{T}}$, $\lambda = [\lambda_1 \ \lambda_2 \ \lambda_3]^{\mathrm{T}}$, and then we have $\zeta = S^{-1}(\lambda)$. The derivative of ζ_i can be obtained as

$$\dot{\zeta}_i = \frac{\partial S^{-1}}{\partial \lambda_i}\dot{\lambda}_i = \varpi_i\left(\dot{x}_i - \frac{\dot{\varphi}}{\varphi}x_i\right) \tag{17}$$

where

$$\varpi_i = \frac{1}{2\varphi}\left(\frac{1}{\lambda_i + \underline{\delta}_i} - \frac{1}{\lambda_i - \bar{\delta}_i}\right) > 0 \tag{18}$$

which can be easily proved to be positive and bounded, with

$$\dot{\varphi}(t) = \nu - \nu\coth^2(\nu t + \iota). \tag{19}$$

The second-order changing rate of ζ_i can be calculated as

$$\ddot{\zeta}_i = \dot{\varpi}_i\left(\dot{x}_i - \frac{x_i\dot{\varphi}}{\varphi}\right) + \varpi_i\left[\ddot{x}_i - \left(\frac{\dot{x}_i\dot{\varphi} + x_i\ddot{\varphi}}{\varphi} - \frac{x_i\dot{\varphi}^2}{\varphi^2}\right)\right]. \tag{20}$$

Denote $\Xi = \mathrm{diag}\{\varpi_1, \ \varpi_2, \ \varpi_3\}$, $\dot{\Xi} = \mathrm{diag}\{\dot{\varpi}_1, \ \dot{\varpi}_2, \ \dot{\varpi}_3\}$, then we can respectively rewrite (17) and (20) as

$$\dot{\zeta} = \Xi\left(\varepsilon_2 - \frac{\dot{\varphi}}{\varphi}\varepsilon_1\right) \tag{21}$$

and the second-order derivative of ζ can be deducted as

$$\begin{aligned}
\ddot{\zeta} &= \Xi\dot{\varepsilon}_2 + \dot{\Xi}\left(\dot{\varepsilon}_1 - \frac{\varepsilon_1\dot{\varphi}}{\varphi}\right) + \Xi\left[-\left(\frac{\dot{\varepsilon}_1\dot{\varphi} + \varepsilon_1\ddot{\varphi}}{\varphi} - \frac{\varepsilon_1\dot{\varphi}^2}{\varphi^2}\right)\right] \\
&= \Xi[A_{21}\varepsilon_1 + A_{22}\varepsilon_2 + B_2\mathrm{sat}(u) + E_2 d] \\
&\quad + \dot{\Xi}\left(\dot{\varepsilon}_1 - \frac{\varepsilon_1\dot{\varphi}}{\varphi}\right) + \Xi\left[-\left(\frac{\dot{\varepsilon}_1\dot{\varphi} + \varepsilon_1\ddot{\varphi}}{\varphi} - \frac{\varepsilon_1\dot{\varphi}^2}{\varphi^2}\right)\right] \\
&= F(\varepsilon) + \Xi B_2 u + \Xi E_2 d
\end{aligned} \tag{22}$$

where

$$F(\varepsilon) = \left(\Xi A_{21} - \dot{\Xi}\frac{\dot{\varphi}}{\varphi} - \Xi\frac{\ddot{\varphi}}{\varphi} + \Xi\frac{\dot{\varphi}^2}{\varphi^2}\right)\varepsilon_1 + \left(\Xi A_{22} + \dot{\Xi} - \Xi\frac{\dot{\varphi}}{\varphi}\right)\varepsilon_2.$$

B. PPF and Simplified NN-Based RISE Control Design

After the error transformation with the proposed PPF is implemented, we will continue to construct the RISE controller, in which a simplified NN estimator is proposed to approximate the unknown disturbance caused by the vehicle vertical dynamics. Denote $z_1 = \zeta$, and define the RISE control variables as

$$z_2 = \dot{z}_1 + k_1 z_1, \quad r = \dot{z}_2 + k_2 z_2 \tag{23}$$

where $k_i = \mathrm{diag}\{k_{i1}, \ k_{i2}, \ k_{i3}\}$ $(i = 1, \ 2)$ are the positive constants selected by the designers. Then, we have

$$\begin{aligned}
r &= \ddot{z}_1 + k_1\dot{z}_1 + k_2 z_2 \\
&= F(\varepsilon) + \Xi B_2 u + \Xi E_2 d + k_1 \Xi\left(\varepsilon_2 - \frac{\dot{\varphi}}{\varphi}\varepsilon_1\right) + k_2 z_2.
\end{aligned} \tag{24}$$

Note that there is a time-varying item ΞB_2 multiplied with the input u in (24), and by differentiating r there will be u and its time derivative, which is complex for the controller design. To overcome this difficulty, the following normalization is implemented:

$$\begin{aligned}
\Xi^{-1}r &= \Xi^{-1}\left[F(\varepsilon) + k_1 \Xi\left(\varepsilon_2 - \frac{\dot{\varphi}}{\varphi}\varepsilon_1\right) + k_2 z_2\right] \\
&\quad + B_2 u + E_2 d.
\end{aligned} \tag{25}$$

Denote

$$S = \Xi^{-1}\left[F(\varepsilon) + k_1 \Xi\left(\varepsilon_2 - \frac{\dot{\varphi}}{\varphi}\varepsilon_1\right) + k_2 z_2\right], d_n = E_2 d \tag{26}$$

then we have

$$\Xi^{-1}r = S + B_2 u + d_n \tag{27}$$

whose time derivative can be obtained as

$$\frac{d(\Xi^{-1}r)}{dt} = \dot{S} + B_2\dot{u} + \dot{d}_n. \tag{28}$$

Since $d(\Xi^{-1}r)/dt = -\Xi^{-1}\dot{\Xi}\Xi^{-1}r + \Xi^{-1}\dot{r}$, according to the above two equations, we have

$$\begin{aligned}
\Xi^{-1}\dot{r} &= d(\Xi^{-1}r)/dt + \Xi^{-1}\dot{\Xi}\Xi^{-1}r \\
&= \dot{S} + B_2\dot{u} + \dot{d}_n + \Xi^{-1}\dot{\Xi}\Xi^{-1}r.
\end{aligned} \tag{29}$$

The structure of adopted RBFNN is a three-layer feedforward network shown as in Fig. 5, where N is the number of output

This article has been accepted for inclusion in a future issue of this journal. Content is final as presented, with the exception of pagination.

HU *et al.*: RISE-BASED INTEGRATED MOTION CONTROL OF AGVs WITH ASYMPTOTIC PRESCRIBED PERFORMANCE
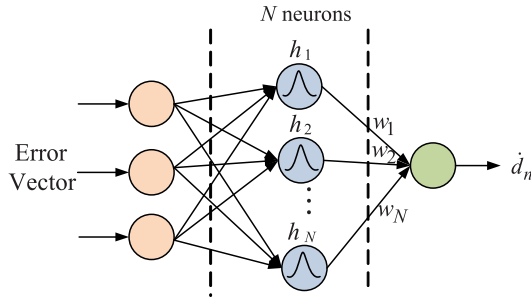
7

Fig. 5.   Structure of adopted RBFNN.

node. Traditionally, we need to use the following expression of NN to approximate the unknown disturbance item $\dot{d}_n$ as:

$$\dot{d}_n = W^{\mathrm{T}}h(\zeta) + \xi \tag{30}$$

where $W = [W_1, \ W_2, \ W_3]$, $W_i = [W_{i1}, \ldots, W_{iN}]^{\mathrm{T}}$, $(i = 1, \ 2, \ 3)$ is the bounded NN weight vector, while we can also denote $W^T = [w_1 \ w_2 \ \cdots \ w_N]$. $h = [h_1 \ h_2 \ \cdots \ h_N]^T$ is the regressor vector, $\xi = [\xi_1 \ \xi_2 \ \xi_3]^T$ is a bounded approximation error. $h_i(\zeta)$ is the Gaussian function selected as

$$h_j(\zeta) = \exp\left(-\frac{\|\zeta - C_j\|^2}{\theta_j^2}\right), \quad j = 1, \ 2, \ldots, \ N \tag{31}$$

where $C_j = [c_{j1}, \ c_{j2}, \ c_{j3}]^T$ is the center of the receptive field, θ_j is the width of the Gaussian function. In this article, we have chose $N = 5$. This strategy has been widely used in the area of autonomous vehicles and automotive system to approximate the unknown disturbances or uncertainties [48]–[50]. Equation (30) shows the structure of the NN approach in terms of approximating the unknown disturbances, and (31) represents the standard Gaussian function expression, which is the standard and formal procedures in this approach.

The ideal RBFNN weight vector W_i is bounded as $\|W_i\| \leq \omega_{\max i}$, $\omega_{\max i} > 0$. To simplify the computational procedure, we define a positive constant as follows: $\omega_i = \|W_i\|^2$. Since $\|W_i\| \leq \omega_{\max i}$, ω_i is obviously bounded. Let $\hat{\omega}_i$ will be the estimate of ω_i, and $\tilde{\omega}_i = \omega_i - \hat{\omega}_i$. The norm of ideal RBFNN weight vector W_i will be estimated via $\hat{\omega}_i$ in following design, which will effectively simplify the NN process.

Deign the RISE controller as

$$u = -B_2^{-1}\left[u_s + \int_0^t \frac{1}{2}\hat{\Omega}rh^T(\zeta)h(\zeta)d\tau\right] \tag{32}$$

where

$$u_s = (k_s + 2)z_2 - (k_s + 2)z_2(0)$$
$$+ \int_0^t \left[(k_s + 2)k_2 z_2 - \beta_1 \mathrm{sgn}(z_2)\right]d\tau \tag{33}$$

which denotes the robust feedback term, k_s and β_1 are positive feedback gains, $\hat{\Omega} = \mathrm{diag}\{\hat{\omega}_1, \ \hat{\omega}_2, \ \hat{\omega}_3\}$, and NN weight $\hat{\omega}_i$ can be updated by using the following adaptive law:

$$\dot{\hat{\omega}}_i = \frac{1}{2}\gamma_i z_{2i}^T r_i h^T h - \kappa_i \gamma_i \hat{\omega}_i \ (i = 1, \ 2, \ 3) \tag{34}$$

where $\gamma_i > 0$ is the learning gain, and κ_i is the forgetting factor. Note that the NN weights are updated online according

to the tracking error z_2, thus the need of offline training process is canceled.

Taking the derivative of the controller, we have

$$\dot{u} = -B_2^{-1}\left(\frac{1}{2}\hat{\Omega}rh^Th + \dot{u}_s\right)$$
$$\dot{u}_s = (k_s + 2)r - \beta_1 \mathrm{sgn}(z_2). \tag{35}$$

By substituting the proposed controller (35) into the control system (29), we have

$$\Xi^{-1}\dot{r} = \frac{1}{2}\tilde{\Omega}rh^Th - (k_s + 2)r + \beta_1 \mathrm{sgn}(z_2)$$
$$+ \dot{S} + \Xi^{-1}\dot{\Xi}\Xi^{-1}r + \xi \tag{36}$$

from which we can obtain the following lemma.

Lemma 2: The closed-loop system of r with the proposed controller can be described as

$$\Xi^{-1}\dot{r} = \tilde{N} + N - z_2 - (k_s + 1)r$$
$$+ \beta_1 \mathrm{sgn}(z_2) + \frac{1}{2}\Xi^{-1}\dot{\Xi}\Xi^{-1}r \tag{37}$$

where

$$\tilde{N} = \dot{S} + z_2 - r + \frac{1}{2}\Xi^{-1}\dot{\Xi}\Xi^{-1}r$$
$$N = N_B + N_d, \quad N_B = \frac{1}{2}\tilde{\Omega}rh^Th, \quad N_d = \xi. \tag{38}$$

According to the theoretical analysis shown in [51], mean value theorem is applied to the function $\tilde{N}$, which is continuously differentiable. Then it can be proved that $\tilde{N}$ is bounded as $\|\tilde{N}(t)\| \leq \rho(\|\eta\|)\|\eta\|$, where $\eta(t) = [z_1 \ z_2 \ r]^T$ and the function $\rho(\|\eta\|) \in R$ is a globally positive and invertible nondecreasing function. Moreover, according to the above inequalities and analysis in [51], N_B, N_d and their changing rates are bounded by

$$\|N_B\| \leq \varsigma_{N_{B0}}, \quad \|\dot{N}_B\| \leq \varsigma_{N_{B1}} + \varsigma_{N_{B2}}\|z_2\|$$
$$\|N_d\| \leq \varsigma_{N_{d1}}, \quad \|\dot{N}_d\| \leq \varsigma_{N_{d2}} \tag{39}$$

where $\varsigma_{N_{B0}}$, $\varsigma_{N_{B1}}$, $\varsigma_{N_{B2}}$, $\varsigma_{N_{d1}}$, and $\varsigma_{N_{d2}}$ are positive constants.

Lemma 3 [26]: Define an auxiliary function $L(t)$ as

$$L(t) = r^{\mathrm{T}}[N_B + N_d + \beta_1 \mathrm{sgn}(z_2)]$$
$$+ \sum_{i=1}^{3} \frac{\kappa_i \|\omega_i\|^2}{4} - \beta_2 \|z_2\|^2 - z_2 N_B \tag{40}$$

where β_1 and β_2 are positive tuning parameters introduced in (33) and (40), which are appropriately selected to satisfy the following requirements:

$$\beta_1 > \varsigma_{N_{B0}} + \varsigma_{N_{d1}} + (\varsigma_{N_{B1}} + \varsigma_{N_{d2}})/k_2, \quad \beta_2 > \varsigma_{N_{B2}}. \tag{41}$$

Then the following inequality can be achieved as:

$$\int_0^t L(\tau)d\tau \leq \beta_1 \|z_2(0)\| - z_2(N_B(0) + N_d(0)). \tag{42}$$

Lemma 2's proof can be secured by virtue of the proof in [26]. The main results of the RISE controller design can now be summarized as follows.

Theorem 1: Consider the vehicle lane keeping and roll dynamics given by (9), under the controller given in (32)

with the modified NN weight updated in (34), the closed-loop system is semiglobally stable. Furthermore, the tracking errors asymptotically converge to zero (i.e., $\|\varepsilon_1(t)\| \to 0$ as $t \to \infty$), and the transient trajectory of $\varepsilon_1(t)$ can be maintained in the prescribed performance constraints (10).

Proof: Define an auxiliary function $P(t)$ as $\dot{P}(t) = -L(t)$. A Lyapunov function is chosen as

$$V_L = \frac{1}{2} z_1^{\mathrm{T}} z_1 + \frac{1}{2} z_2^{\mathrm{T}} z_2 + \frac{1}{2} r^{\mathrm{T}} \Xi^{-1} r + Q + P \qquad (43)$$

with $Q = (1/2) \sum_{i=1}^{3} (1/\gamma_i) \tilde{\omega}_i^2$. V_L satisfies the following inequalities:

$$U_1(y) \le V_L(y) \le U_2(y) \qquad (44)$$

where $y = [z_1^T, z_2^T, r^T, \sqrt{Q}, \sqrt{P}]^T$, and $U_1(y)$ and $U_2(y)$ are defined as $U_1(y) = \lambda_{c1} \|y\|^2$, $U_2(y) = \lambda_{c2} \|y\|^2$, with λ_{c1} and λ_{c2} being positive constants. According to

$$\frac{d(r^T \Xi^{-1} r)}{dt} = 2 r^T \Xi^{-1} \dot{r} + r^T \frac{d(\Xi^{-1})}{dt} r, \quad \frac{d(\Xi^{-1})}{dt} = -\Xi^{-1} \dot{\Xi} \Xi^{-1}. \qquad (45)$$

Based on Lemmas 2 and 3, the time derivative of V_L can be expressed as

$$
\begin{aligned}
\dot{V}_L &= z_1^T \dot{z}_1 + z_2^T \dot{z}_2 + r^T \Xi^{-1} \dot{r} - \frac{1}{2} r^T \Xi^{-1} \dot{\Xi} \Xi^{-1} r + \dot{Q} + \dot{P} \\
&= z_1^T (z_2 - k_1 z_1) + z_2^T (r - k_2 z_2) - \frac{1}{2} r^T \Xi^{-1} \dot{\Xi} \Xi^{-1} r \\
&\quad + r^T \Big[\tilde{N} + N - z_2 - (k_s + 1) r + \beta_1 \mathrm{sgn}(z_2) \\
&\qquad\qquad + \frac{1}{2} \Xi^{-1} \dot{\Xi} \Xi^{-1} r \Big] + \dot{Q} + \dot{P} \\
&= z_1^T (z_2 - k_1 z_1) + z_2^T (r - k_2 z_2) \\
&\quad + r^T [\tilde{N} + N - (k_s + 1) r + \beta_1 \mathrm{sgn}(z_2) - z_2] \\
&\quad + \sum_{i=1}^{3} \frac{1}{\gamma_i} \tilde{\omega}_i \dot{\tilde{\omega}}_i - r^T [N_B + N_d + \beta_1 \mathrm{sgn}(z_2)] \\
&\quad - \sum_{i=1}^{3} \frac{\kappa_i \|\omega_i\|^2}{4} + \beta_2 \|z_2\|^2 + z_2 N_B \\
&= -k_1 z_1^T z_1 - k_2 z_2^T z_2 + z_1^T z_2 - (k_s + 1) r^T r + \beta_2 \|z_2\|^2 \\
&\quad + r^T \tilde{N} + z_2 N_B + \sum_{i=1}^{3} \frac{1}{\gamma_i} \tilde{\omega}_i \dot{\tilde{\omega}}_i - \sum_{i=1}^{3} \frac{\kappa_i \|\omega_i\|^2}{4}. \qquad (46)
\end{aligned}
$$

Substituting the adaptive law (34) into $\tilde{W}^{\mathrm{T}} \Gamma^{-1} \dot{\tilde{W}}$, we have

$$\sum_{i=1}^{3} \frac{1}{\gamma_i} \tilde{\omega}_i \dot{\tilde{\omega}}_i = -\sum_{i=1}^{3} \left(\frac{1}{2} \tilde{\omega}_i z_{2i}^T r_i h^T h - \kappa_i \tilde{\omega}_i \hat{\omega}_i \right). \qquad (47)$$

Considering the expression of N_B, we have

$$
\begin{aligned}
&z_2^T N_B + \sum_{i=1}^{3} \frac{1}{\gamma_i} \tilde{\omega}_i \dot{\tilde{\omega}}_i \\
&= \frac{1}{2} z_2^T \tilde{\Omega} r h^T h - \sum_{i=1}^{3} \left(\frac{1}{2} \tilde{\omega}_i z_{2i}^T r_i h^T h - \kappa_i \tilde{\omega}_i \hat{\omega}_i \right)
\end{aligned}
$$

$$= \sum_{i=1}^{3} \kappa_i \tilde{\omega}_i \hat{\omega}_i \qquad (48)$$

then we have

$$
\begin{aligned}
\dot{V}_L &= -k_1 z_1^{\mathrm{T}} z_1 - k_2 z_2^{\mathrm{T}} z_2 + z_1^{\mathrm{T}} z_2 - (k_s + 1) r^T r + \beta_2 \|z_2\|^2 \\
&\quad + r^T \tilde{N} + \sum_{i=1}^{3} (\kappa_i \tilde{\omega}_i \hat{\omega}_i) - \sum_{i=1}^{3} \frac{\kappa_i \|\omega_i\|^2}{4}. \qquad (49)
\end{aligned}
$$

With the Young's inequality, we have

$$
\begin{aligned}
\sum_{i=1}^{3} (\kappa_i \tilde{\omega}_i \hat{\omega}_i) &= \sum_{i=1}^{3} (-\kappa_i \tilde{\omega}_i \tilde{\omega}_i + \kappa_i \tilde{\omega}_i \omega_i) \\
&\le \sum_{i=1}^{3} \left[-\kappa_i \left(\|\tilde{\omega}_i\| - \frac{\|\omega_i\|}{2} \right)^2 + \frac{\kappa_i \|\omega_i\|^2}{4} \right] \qquad (50)
\end{aligned}
$$

and

$$
\begin{aligned}
-k_s r^T r + r^T \tilde{N} &\le -k_s r^T r + \|r\| \rho(\|\eta\|) \|\eta\| \\
&\le \frac{\rho^2(\|\eta\|) \|\eta\|^2}{4 k_s} \qquad (51)
\end{aligned}
$$

so we have

$$
\begin{aligned}
\dot{V}_L &\le -\left(k_1 - \frac{1}{2} \right) z_1^T z_1 - \left(k_2 - \frac{1}{2} - \beta_2 \right) z_2^T z_2 \\
&\quad - \sum_{i=1}^{3} \left[\kappa_i \left(\|\tilde{\omega}_i\| - \frac{1}{2} \|\omega_i\| \right)^2 \right] - (k_s + 1) r^T r + r^T \tilde{N} \\
&\le -\lambda_{c3} \|\eta\|^2 + \frac{\rho^2(\|z\|)}{4 k_s} \|\eta\|^2 \\
&\quad - \sum_{i=1}^{3} \left[\kappa_i \left(\|\tilde{\omega}_i\| - \frac{1}{2} \|\omega_i\| \right)^2 \right] \\
&\le -\lambda_{c3} \|\eta\|^2 + \frac{\rho^2(\|\eta\|) \|\eta\|^2}{4 k_s} \le -c \|\eta\|^2 \qquad (52)
\end{aligned}
$$

for $\|\eta\| < \rho^{-1}(2\sqrt{\lambda_{c3} k_s})$, where c is a positive constant, and $\lambda_{c3} = \min\{(k_1 - (1/2)), \quad (k_2 - (1/2) - \beta_2), \quad 1\}$. $c\|\eta\|$ is considered as a continuous positive semidefinite function $U(y)$ which is defined on the following set:

$$\mathcal{D} = \left\{ y \in \Re^5 | \|y\| \le \rho^{-1} \left(2 \sqrt{\lambda_{c3} k_s} \right) \right\}. \qquad (53)$$

Therefore, inequalities (44) and (52) can be used to show that $V_L \in L_\infty$ over $\mathcal{D}$, which further implies that z_1, z_2, $P(t)$, $Q(t)$, and $r(t) \in L_\infty$. Moreover, the following results can be obtained based on the definition of RISE:

$$\|z_1\|, \|z_2\| \to 0 \text{ when } t \to \infty \ \forall \ y(0) \in \mathcal{D}.$$

Based on the error transformation (16), we can easily obtain

$$\lambda \to 0 \text{ when } t \to \infty \ \forall \ y(0) \in \mathcal{D}$$

which means the controlled system states can be asymptotically converged to zero within the proposed PPF constraints.

According to Lemma 1 in the revised paper, the prescribed performance constraint (10) can be guaranteed if the transformed error ζ_i is bounded and the initial value of the controlled state $x_i(0)$ is always within the performance bounds, i.e., $-\underline{\delta}_i \varphi(0) < x_i(0) < -\bar{\delta}_i \varphi(0)$, and therefore the *Theorem 1* can guarantee that the transformed error ζ_i is bounded.
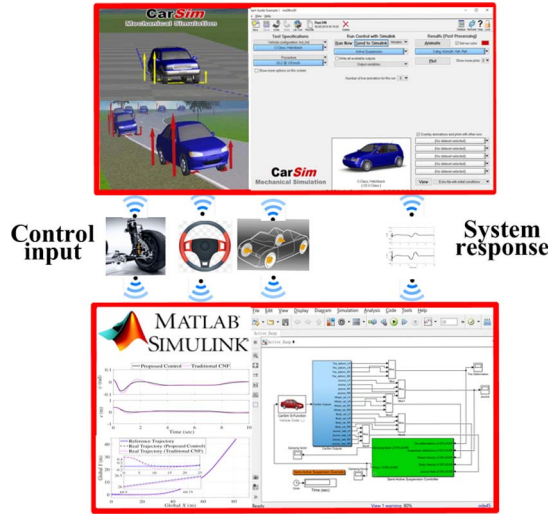
Fig. 6. Schematic of the high-fidelity CarSim-MATLAB platform.

TABLE I
VEHICLE PARAMETERS USED IN THE SIMULATION

Definition and Symbol	Value
Total Vehicle mass m	1832 kg
Vehicle sprung mass m_s	1592 kg
Left unsprung mass of the vehicle m_{f1}	60 kg
Right unsprung mass of the vehicle m_{f2}	60 kg
Left tire vertical stiffness k_{t1}	230000 N/m
Right tire vertical stiffness k_{t2}	230000 N/m
Left suspension stiffness k_{s1}	146000 N/m
Right suspension stiffness k_{s2}	146000 N/m
Left suspension damping coefficient c_{p1}	3000 N/m
Right suspension damping coefficient c_{p2}	3000 N/m
Moment of inertia about Z axis I_z	2488 kg $\cdot$ m^2
Moment of inertia about X axis I_x	614 kg $\cdot$ m^2
Half of wheel track l_s	0.7875 m
Distance between the roll center to the CG of the sprung mass h_r	0.5 m
Distance of CG from front axle l_f	1.18 m
Distance of CG from rear axle l_r	1.77 m
Cornering stiffness of front tires c_f	80000 N/rad
Cornering stiffness of rear tires c_r	80000 N/rad

IV. SIMULATION STUDY

In this section, CarSim–Simulink simulations with a high-fidelity and full-car model have been conducted to verify the effectiveness of the proposed RISE controller. The schematic diagram of the high-fidelity CarSim–Simulink simulation platform is shown in Fig. 6. The practical road environment, a nonlinear and high-fidelity SUV model, and actual driving maneuvers are embedded in this platform, where the measured state signal is transferred into the Simulink module for generating the control signal. As a consequence, the vehicle and tire models used in the simulations have incorporated the nonlinearities, system uncertainties, and external disturbances. The vehicle parameters used in the simulations are shown in Table I [52]. Two driving maneuvers with different speeds and road adhesion conditions are implemented in the simulation, including the J-turn and S-turn cases. The control purpose is to make the vehicle complete the required maneuver and maintain the roll stability with guaranteed prescribed performance.

Considering the physical limitation of the actuators, the constraints of steering angle δ_f, external yaw moment ΔM_z, and external roll moment ΔM_x are chosen as 0.2 rad, 3000 N $\cdot$ m, and 3000 N $\cdot$ m, respectively. The PPF gains are chosen as $\bar{\delta} = \underline{\delta} = [1.5, 1, 1]$, $\nu = [1.2, 1.4, 1.4]$, and $\iota = [0.6, 1.3, 1.3]$. The controller gains are $k_1 = \mathrm{diag}\{0.5, 1.2, 3.1\}$, $k_2 = \mathrm{diag}\{0.2, 0.8, 1.6\}$, $k_3 = \mathrm{diag}\{0.9, 0.6, 2.2\}$, and $\beta_1 = [0.3, 0.6, 1.4]$. As for the NN observer, $\Gamma = [12, 16, 2.6]$ and $\kappa = [4.5, 11, 7]$. The initial values of e and ψ are selected as 0.5 m and -0.05 rad. The initial values of the roll angle and roll rate are assumed as zero. To verify the superiority of the proposed approach, we have compared the proposed controller with a multivariable SMC controller based on the super-twisting algorithm proposed in [53], which is denoted as "MVSMC" in the results.

A. J-Turn Simulation

In the J-Turn simulation, the vehicle runs with a low speed, $v_x = 10$ m/s on a slippery road ($\mu = 0.4$, where μ is the tire-road friction coefficient), and is supposed to make a J-turn maneuver automatically.
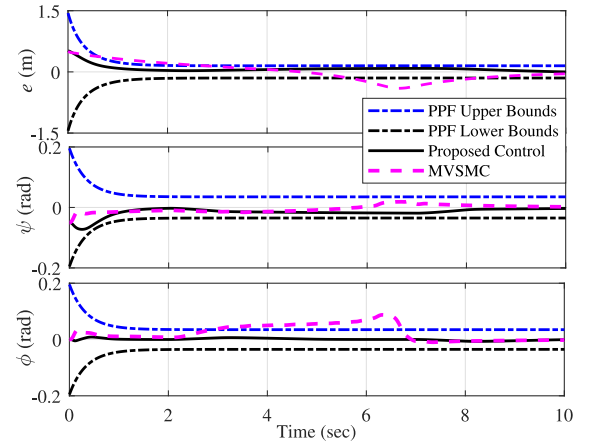

Fig. 7. Lane-keeping errors and roll angle in the J-Turn simulation.

The lane-keeping errors and the roll angle in the J-Turn simulation are shown in Fig. 7. From the results, one can find both the proposed controller and traditional MVSMC controller can stabilize the trajectory-tracking errors. However, the former can apparently yield better transient tracking performance by effectively lowering the overshoots and oscillations in the responses, and more importantly, confining the trajectory within the prescribed performance boundaries. While the trajectories easily exceed the PPF bounds and have a slow rise time and large steady-state errors using the traditional MVSMC approach. It can be seen obviously that the roll angle has large overshoot during 6 and 7 s, which is very easy to cause a rollover. Note that with the proposed controller, the lateral offset can be maintained to stay at zero, but there is a tiny steady-state value for the heading error. That is because of the sideslip angle usually exists in the steering maneuvers, which is necessary to guarantee the turning smoothness in curve followings [54].

The three key vehicle states, including the roll rate, yaw rate, and sideslip angle are presented in Fig. 8. It is found that the changing trends of these variables coincide with that of the road curvature. They are maintained in reasonable and
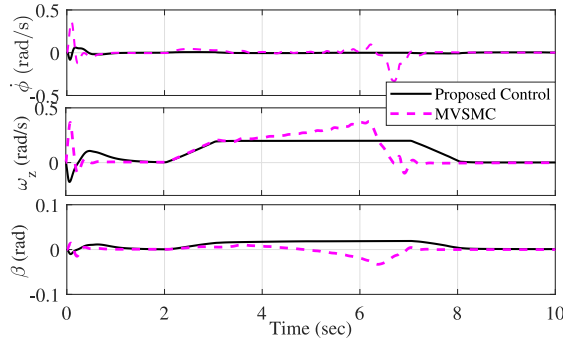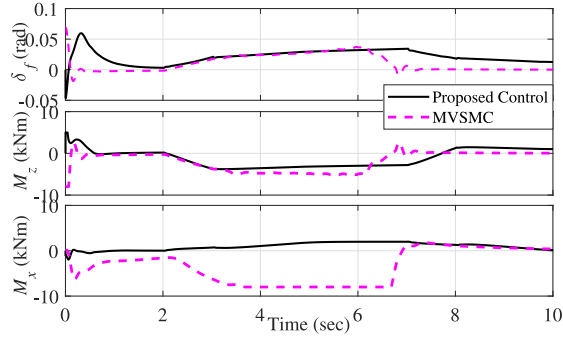
Fig. 8.   Vehicle states in the J-Turn simulation.

Fig. 9.   Control inputs in the LC simulation.

Fig. 10.   Global Trajectory in the J-Turn simulation.

Fig. 11.   Lane-keeping errors and roll angle in the S-turn simulation.

sufficiently small and reasonable regions in the steady state by using both methods. Similarly, it can be found that the vehicle states have higher performances, including more smooth responses and lower overshoots by using the developed controller comparing with the MVSMC approach. It is inferred that the lateral stability is ensured according to the magnitude of the sideslip angle. However, there is an obvious oscillation for the roll rate during 6–7 s using the MVMSC approach, which is very dangerous for the vehicle roll stability. Also, it is observed in the case of the MVSMC, those vehicle states have distinctly large overshoots in the initial phase. It is obvious that the developed controller can effectively enhance the transient performance of the controlled vehicle states, which have important impacts on vehicle stability, safety, and ride comfort.

The results of the control inputs are presented in Fig. 9, including the steering angle, external yaw moment, and external roll moment. They are all maintained in rational regions by using both controllers. Note that in the slippery road the control inputs should be sufficiently small to guarantee the vehicle lateral and roll stability. It is found the developed control strategy can successfully restrain the magnitudes of the control inputs, and also effectively reduce their overshoots and oscillations. However, by using the MVSMC, the input signals have large overshoots and thus may easily exceed the actuator constraints, which will be very likely to deteriorate the overall control performance. Some oscillations on the proposed control inputs are admissible and reasonable, which results from the fact that the PPF constraints applied in the control loop are dramatically and exponentially decreasing in the initial phase.
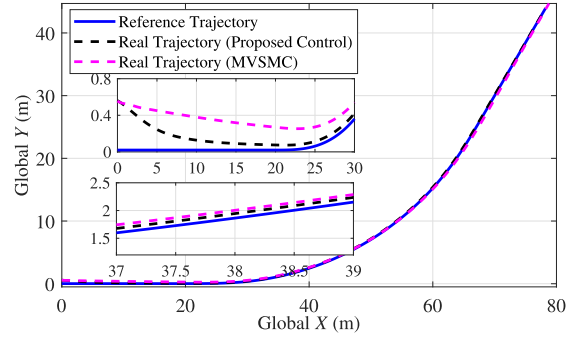
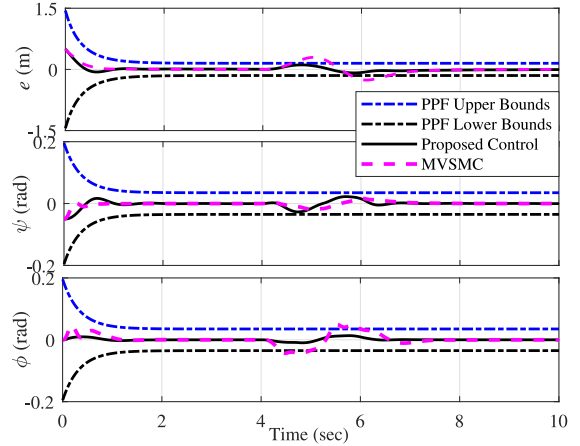The global motion trajectory of the J-turn maneuver is shown in Fig. 10. From the result, one can easily observe that the developed control approach can make the J-turn maneuver completed more fast and accurate with better performance, which actually can even be prescribed. However, using the MVSMC strategy, we find the overall trajectory tracking control has large errors with inferior performance, which might exert a safety hazard to the vehicle. It can be concluded that the developed controller can considerably enhance the transient performance of the lane-keeping maneuver through restricting the controlled outputs within the asymptotic PPF constraint bounds for the driving in the slippery roads.

B. S-Turn Simulation

In the second simulation, the vehicle travels with a high speed ($v_x = 30$ m/s) on a dry road ($\mu = 0.8$). S-turn (or lane change) is a highly frequent but dangerous maneuver in highways, which is likely to cause the lateral slip or rollover. So in this simulation case, the vehicle is made to make a S-turn with high speed in about 3 s.

The results of the lane-keeping errors and roll angle are shown in Fig. 11. It can be seen that they are all stabilized and converged to zero by the two controllers. However, it is found that the controlled stated can be restricted in the prescribed performance bounds and have fewer oscillations, smaller overshoots, and steady-state errors by using the developed control, while they easily surpass the prescribed
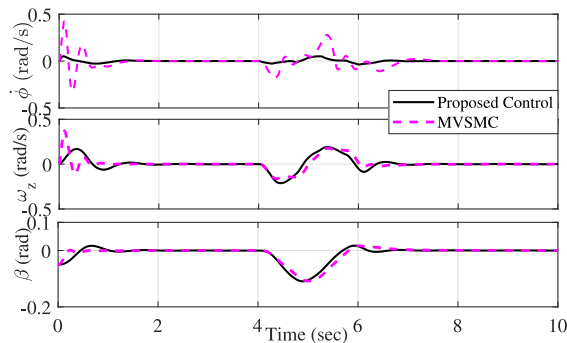
This article has been accepted for inclusion in a future issue of this journal. Content is final as presented, with the exception of pagination.

HU *et al.*: RISE-BASED INTEGRATED MOTION CONTROL OF AGVs WITH ASYMPTOTIC PRESCRIBED PERFORMANCE 11

Fig. 12. Vehicle states in the S-turn simulation.

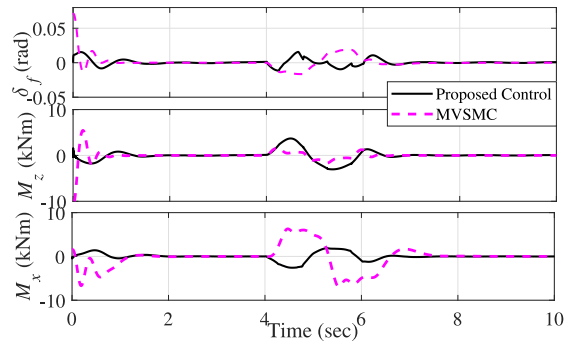Fig. 14. Global trajectory in the S-turn simulation.

Fig. 13. Control inputs in the S-turn simulation.

performance bounds and have large steady-state errors, slow rise time if the MVSMC is applied. The response of the roll angle has shown that the roll stability of the vehicle is guaranteed during the simulations. There are some errors in the controlled states during the lane-change maneuver, which is normal, as the path curvature is dramatically changing.

The vehicle states are shown in Fig. 12. These signals are all maintained in reasonable regions in the steady state, and change with the variation of the road curvature. According to the magnitude of the sideslip angle, the vehicle lateral stability is guaranteed. They have large initial overshoots and oscillations with the MVSMC approach. It can be clearly seen that the developed control strategy can restrain the overshoots and oscillations in these states, and restrict them in safe boundaries. In the steady state, their values are similar with difference control strategies. Especially, the roll rate has large oscillations during 4–7 s using MVMSC approach, exerting great risk of the rollover. The control inputs are shown in Fig. 13. From the results, we find the control inputs of the two control approaches have both been retained in reasonable regions. To prevent the vehicle from slipping or roller, the steering angle is maintained within a small magnitude when the vehicle is conducting an S-turn. One can obviously find that the developed control strategy can considerably suppress the overshoots and shakes on the control input signals, and thus generate a more smooth input for the system so as to reduce the chattering effects.

The vehicle global trajectory is shown in Fig. 14. From this figure, we can clearly see that by using the developed control, the vehicle can achieve a more fast and accurate S-turn
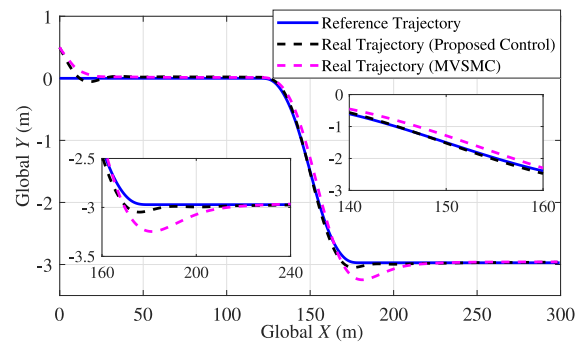
manoeuver with small overshoots and oscillations compared with the MVSMC. Till now it can be concluded that the developed control of this article can effectively achieve the S-turn and roll control with asymptotic convergence property, and maintain the controlled variables within PPF bounds in the presence of unknown suspension disturbances in different driving and road conditions.

V. CONCLUSION

This article investigated the robust lane keeping and roll control for AGVs in the presence of unknown suspension disturbances. An enhanced RISE control strategy is developed to achieve the control objective, realize the asymptotic stability of the closed-loop system, and attenuate unknown disturbance, which incorporating the merit of the PPC in prescribing the transient tracking control performance. A modified PPF is developed to remove the requirement on the initial errors, and a simplified NN approach is presented to reduce the adaption parameters thus alleviate the computation effort for the practical implementation. Finally the PPF and NN are incorporated in the RISE control framework to achieve the control objective, and guarantee both the asymptotic stability of the closed-loop system and the prescribed performance of the transient tracking errors. High-fidelity simulations have verified the superiority of the developed control strategy compared with the MVSMC approach. In our future work, we will investigate how to achieve the rollover prevention when the vehicle enters the nonlinear region, where we should use a nonlinear vehicle dynamics model.

REFERENCES

[1] H. Guo, C. Shen, H. Zhang, H. Chen, and R. Jia, "Simultaneous trajectory planning and tracking using an MPC method for cyber-physical systems: A case study of obstacle avoidance for an intelligent vehicle," *IEEE Trans. Ind. Informat.*, vol. 14, no. 9, pp. 4273–4283, Sep. 2018.

[2] J. Na, A. S. Chen, G. Herrmann, R. Burke, and C. Brace, "Vehicle engine torque estimation via unknown input observer and adaptive parameter estimation," *IEEE Trans. Veh. Technol.*, vol. 67, no. 1, pp. 409–422, Jan. 2018.

[3] J. Peng, Y. Zhou, and C. L. P. Chen, "Region-kernel-based support vector machines for hyperspectral image classification," *IEEE Trans. Geosci. Remote Sens.*, vol. 53, no. 9, pp. 4810–4824, Sep. 2015.

[4] C. Hu, H. Jing, R. Wang, F. Yan, and M. Chadli, "Robust H_∞ output-feedback control for path following of autonomous ground vehicles," *Mech. Syst. Signal Process.*, vols. 70–71, pp. 414–427, Mar. 2016.

[5] L. Guo, H. Chen, Q. F. Liu, and B. Gao, "A computationally efficient and hierarchical control strategy for velocity optimization of on-road vehicles," *IEEE Trans. Syst., Man, Cybern., Syst.*, vol. 49, no. 1, pp. 31–41, Jan. 2019.

[6] X. Tang, X. Hu, W. Yang, and H. Yu, "Novel torsional vibration modeling and assessment of a power-split hybrid electric vehicle equipped with a dual-mass flywheel," *IEEE Trans. Veh. Technol.*, vol. 67, no. 3, pp. 1990–2000, Mar. 2018.

[7] X. Tang, D. Zhang, T. Liu, A. Khajepour, H. Yu, and H. Wang, "Research on the energy control of a dual-motor hybrid vehicle during engine start-stop process," *Energy*, vol. 166, pp. 1181–1193, Jan. 2019.

[8] Y. Wang, J. Gao, K. Li, and H. Chen, "Integrated design of control allocation and triple-step control for over-actuated electric ground vehicles with actuator faults," *J. Frankl. Inst.*, Sep. 2019. [Online]. Available: https://www.sciencedirect.com/science/article/pii/S0016003219305642, doi: 10.1016/j.jfranklin.2019.07.035.

[9] Y. Wang, C. Zong, K. Li, and H. Chen, "Fault-tolerant control for in-wheel-motor-driven electric ground vehicles in discrete time," *Mech. Syst. Signal Process.*, vol. 121, pp. 441–454, Apr. 2019.

[10] Y. Huang *et al.*, "A motion planning and tracking framework for autonomous vehicles based on artificial potential field-elaborated resistance network (APFE-RN) approach," *IEEE Trans. Ind. Electron.*, vol. 67, no. 2, pp. 1376–1386, Feb. 2019. [Online]. Available: https://www.sciencedirect.com/science/article/pii/S0016003219305642

[11] J. Zhao, P. K. Wong, X. Ma, and Z. Xie, "Chassis integrated control for active suspension active front steering and direct yaw moment systems using hierarchical strategy," *Veh. Syst. Dyn.*, vol. 55, no. 1, pp. 72–103, 2017.

[12] H. Guo, F. Liu, F. Xu, H. Chen, D. Cao, and Y. Ji, "Nonlinear model predictive lateral stability control of active chassis for intelligent vehicles and its FPGA implementation," *IEEE Trans. Syst., Man, Cybern., Syst.*, vol. 49, no. 1, pp. 2–13, Jan. 2019.

[13] Y. Qin, C. He, X. Shao, H. Du, C. Xiang, and M. Dong, "Vibration mitigation for in-wheel switched reluctance motor driven electric vehicle with dynamic vibration absorbing structures," *J. Sound Vib.*, vol. 419, pp. 249–267, Apr. 2018.

[14] C. Hu *et al.*, "Lane keeping of autonomous vehicles based on differential steering with adaptive multivariable super-twisting control," *Mech. Syst. Signal Process.*, vol. 125, pp. 330–346, Jun. 2019.

[15] C. Chen, C. Wen, Z. Liu, K. Xie, Y. Zhang, and C. L. P. Chen, "Adaptive consensus of nonlinear multi-agent systems with non-identical partially unknown control directions and bounded modelling errors," *IEEE Trans. Autom. Control*, vol. 62, no. 9, pp. 4654–4659, Sep. 2017.

[16] X. Ma, P. K. Wong, J. Zhao, and Z. Xie, "Cornering stability control for vehicles with active front steering system using T–S fuzzy based sliding mode control strategy," *Mech. Syst. Signal Process.*, vol. 125, pp. 347–364, Feb. 2019.

[17] Y. S. Son, W. Kim, S.-H. Lee, and C. C. Chung, "Robust multirate control scheme with predictive virtual lanes for lane-keeping system of autonomous highway driving," *IEEE Trans. Veh. Technol.*, vol. 64, no. 8, pp. 3378–3391, Aug. 2015.

[18] L. Zhang, H. Ding, Y. Huang, H. Chen, K. Guo, and Q. Li, "An analytical approach to improve vehicle maneuverability via torque vectoring control: Theoretical study and experimental validation," *IEEE Trans. Veh. Technol.*, vol. 68, no. 5, pp. 4514–4526, May 2019.

[19] A. Merah, K. Hartani, and A. Draou, "A new shared control for lane keeping and road departure prevention," *Veh. Syst. Dyn.*, vol. 54, no. 1, pp. 86–101, 2016.

[20] P. Shu, S. Sagara, Q. Wang, and M. Oya, "Improved adaptive lane-keeping control for four-wheel steering vehicles without lateral velocity measurements," *Int. J. Robust Nonlin. Control*, vol. 27, no. 17, pp. 4154–4168, Apr. 2017.

[21] J. Du, X. Hu, H. Liu, and C. L. P. Chen, "Adaptive robust output feedback control for a marine dynamic positioning system based on a highgain observer," *IEEE Trans. Neural Netw. Learn. Syst.*, vol. 26, no. 11, pp. 2775–2786, Nov. 2015.

[22] H. Dahmani, O. Pagès, and A. E. Hajjaji, "Observer-based state feedback control for vehicle chassis stability in critical situations," *IEEE Trans. Control Syst. Technol.*, vol. 24, no. 2, pp. 636–643, Mar. 2016.

[23] L. Li, Y. Lu, R. Wang, and J. Chen, "A three-dimensional dynamics control framework of vehicle lateral stability and rollover prevention via active braking with MPC," *IEEE Trans. Ind. Electron.*, vol. 64, no. 4, pp. 3389–3401, Apr. 2017.

[24] R. Bencatel, A. Girard, and I. Kolmanovsky, "Reference governor strategies for vehicle rollover avoidance," *IEEE Trans. Control Syst. Technol.*, vol. 26, no. 6, pp. 1954–1969, Nov. 2018, doi: 10.1109/TCST.2017.2753168.

[25] C. Hu, Z. Wang, Y. Qin, Y. Huang, J. Wang, and R. Wang, "Lane keeping control of autonomous vehicles with prescribed performance considering the rollover prevention and input saturation," *IEEE Trans. Intell. Transp. Syst.*, to be published, doi: 10.1109/TITS.2019.2924937.

[26] B. Xian, D. M. Dawson, M. S. de Queiroz, and J. Chen, "A continuous asymptotic tracking control strategy for uncertain nonlinear systems," *IEEE Trans. Autom. Control*, vol. 49, no. 7, pp. 1206–1211, Jul. 2004.

[27] J. Shin, J. Huh, and Y. Park, "Asymptotically stable path following for lateral motion of an unmanned ground vehicle," *Control Eng. Practice*, vol. 40, pp. 102–112, Jul. 2015.

[28] C. Chen, M. Shu, and R. Liu, "Virtual-point-based asymptotic tracking control of 4WS vehicles," *Int. J. Control Autom. Syst.*, vol. 13, no. 2, pp. 371–378, Apr. 2015.

[29] C. Hu, R. Wang, F. Yan, and N. Chen, "Robust composite nonlinear feedback path-following control for underactuated surface vessels with desired-heading amendment," *IEEE Trans. Ind. Electron.*, vol. 63, no. 10, pp. 6386–6394, Oct. 2016.

[30] S. Wang, J. Na, and X. Ren, "RISE-based asymptotic prescribed performance tracking control of nonlinear servo mechanisms," *IEEE Trans. Syst., Man, Cybern. Syst.*, vol. 48, no. 12, pp. 2359–2370, Dec. 2018.

[31] C. P. Bechlioulis and G. A. Rovithakis, "Prescribed performance adaptive control for multi-input–multi-output affine in the control nonlinear systems," *IEEE Trans. Autom. Control*, vol. 55, no. 5, pp. 1220–1226, May 2010.

[32] Y. Huang, J. Na, X. Wu, X. Liu, and Y. Guo, "Adaptive control of nonlinear uncertain active suspension systems with prescribed performance," *ISA Trans.*, vol. 54, pp. 145–155, Jan. 2015.

[33] Z. Zheng and M. Feroskhan, "Path following of a surface vessel with prescribed performance in the presence of input saturation and external disturbances," *IEEE/ASME Trans. Mechatronics*, vol. 22, no. 6, pp. 2564–2575, Dec. 2017.

[34] J. Na, Y. Huang, X. Wu, G. Gao, G. Herrmann, and J. Z. Jiang, "Active adaptive estimation and control for vehicle suspensions with prescribed performance," *IEEE Trans. Control Syst. Technol.*, vol. 26, no. 6, pp. 2063–2077, Nov. 2018.

[35] C. Hua, J. Chen, Y. Li, and L. Li, "Adaptive prescribed performance control of half-car active suspension system with unknown dead-zone input," *Mech. Syst. Signal Process.*, vol. 111, pp. 135–148, Oct. 2018.

[36] S. Shao and M. Chen, "Adaptive neural discrete-time fractional-order control for a UAV system with prescribed performance using disturbance observer," *IEEE Trans. Syst., Man, Cybern., Syst.*, to be published, doi: 10.1109/TSMC.2018.2882153.

[37] C. L. P. Chen and Y.-H. Pao, "An integration of neural network and rule-based systems for design and planning of mechanical assemblies," *IEEE Trans. Syst., Man, Cybern., Syst.*, vol. 23, no. 5, pp. 1359–1371, Sep./Oct. 1993.

[38] M. Wang and A. Yang, "Dynamic learning from adaptive neural control of robot manipulators with prescribed performance," *IEEE Trans. Syst., Man, Cybern., Syst.*, vol. 47, no. 8, pp. 2244–2255, Aug. 2017.

[39] Q. Zhou, H. Li, L. Wang, and R. Lu, "Prescribed performance observer-based adaptive fuzzy control for nonstrict-feedback stochastic nonlinear systems," *IEEE Trans. Syst., Man, Cybern., Syst.*, vol. 48, no. 10, pp. 1747–1758, Oct. 2018.

[40] W. Meng, Q. Yang, J. Si, and Y. Sun, "Adaptive neural control of a class of output-constrained nonaffine systems," *IEEE Trans. Cybern.*, vol. 46, no. 1, pp. 85–95, Jan. 2016.

[41] R. Rajamani, *Vehicle Dynamics and Control*. New York, NY, USA: Springer-Verlag, 2012.

[42] Y. Qin, Z. Wang, C. Xiang, M. Dong, C. Hu, and R. Wang, "A novel global sensitivity analysis on the observation accuracy of the coupled vehicle model," *Veh. Syst. Dyn.*, vol. 57, no. 10, pp. 1445–1466, Sep. 2018.

[43] Z. Wang, Y. Qin, C. Hu, M. Dong, and F. Li, "Fuzzy observerbased prescribed performance control of vehicle roll behavior via controllable damper," *IEEE Access*, vol. 7, pp. 19471–19487, 2019.

[44] K. S. Hong *et al.*, "A new model and an optimal pole-placement control of the Macpherson suspension system," *SAE Trans.*, vol. 108, pp. 2452–2461, Jan. 1999.

[45] B. Heissing and M. Ersoy, *Chassis Handbook: Fundamentals, Driving Dynamics, Components, Mechatronics, Perspectives*. New York, NY, USA: Springer, Nov. 2010.

[46] H. Imine and M. Djemai, "Switched control for reducing impact of vertical forces on road and heavy-vehicle rollover avoidance," *IEEE Trans. Veh. Technol.*, vol. 65, no. 6, pp. 4044–4052, Jun. 2016.

This article has been accepted for inclusion in a future issue of this journal. Content is final as presented, with the exception of pagination.

HU *et al.*: RISE-BASED INTEGRATED MOTION CONTROL OF AGVs WITH ASYMPTOTIC PRESCRIBED PERFORMANCE 13

[47] M. Ghazali, M. Durali, and H. Salarieh, "Path-following in model predictive rollover prevention using front steering and braking," *Veh. Syst. Dyn.*, vol. 55, no. 1, pp. 121–148, Jan. 2017.

[48] S. S. Ge, C. C. Hang, T. H. Lee, and T. Zhang, *Stable Adaptive Neural Network Control*. Boston, MA, USA: Kluwer, 2001.

[49] J. Guo, Y. Luo, and K. Li, "Adaptive neural-network sliding mode cascade architecture of longitudinal tracking control for unmanned vehicles," *Nonlin. Dyn.*, vol. 87, no. 4, pp. 2497–2510, Mar. 2017.

[50] C. Hu *et al.*, "MME-EKF-based path-tracking control of autonomous vehicles considering input saturation," *IEEE Trans. Veh. Technol.*, vol. 68, no. 6, pp. 5246–5259, Jun. 2019.

[51] P. M. Patre, W. MacKunis, K. Kaiser, and W. E. Dixon, "Asymptotic tracking for uncertain dynamic systems via a multilayer neural network feedforward and RISE feedback control structure," *IEEE Trans. Autom. Control*, vol. 53, no. 9, pp. 2180–2185, Oct. 2008.

[52] Z. Wang, Y. Qin, L. Gu, and M. Dong, "Vehicle system state estimation based on adaptive unscented Kalman filtering combing with road classification," *IEEE Access*, vol. 5, pp. 27786–27799, 2017.

[53] I. Nagesh and C. Edwards, "A multivariable super-twisting sliding mode approach," *Automatica*, vol. 50, no. 3, pp. 984–988, Mar. 2014.

[54] C. Hu, R. Wang, F. Yan, and N. Chen, "Should the desired heading in path following of autonomous vehicles be the tangent direction of the desired path?" *IEEE Trans. Intell. Transp. Syst.*, vol. 16, no. 6, pp. 3084–3094, Dec. 2015.

Chuan Hu received the B.E. degree in vehicle engineering from Tsinghua University, Beijing, China, in 2010, the M.E. degree in vehicle operation engineering from the China Academy of Railway Sciences, Beijing, in 2013, and the Ph.D. degree in mechanical engineering from McMaster University, Hamilton, ON, Canada, in 2017.

He is currently a Post-Doctoral Fellow with the Department of Mechanical Engineering, University of Texas at Austin, Austin, TX, USA. He was a Post-Doctoral Fellow with the Department of Systems Design Engineering, University of Waterloo, Waterloo, ON, Canada, from July 2017 to July 2018. His current research interest includes vehicle system dynamics and control, motion control and estimation of autonomous vehicles, mechatronics, and robust and adaptive control.

Hongbo Gao received the Ph.D. degree in autonomous vehicles from Beihang University, Beijing, China, in 2016.

He is currently an Associate Professor with the Department of Automation, School of Information Science and Technology, University of Science and Technology of China, Hefei, China. He has authored or coauthored of over 30 journal papers. He is the co-holder of six patent applications. His current research interests include unmanned system platform and robotics, machine learning, decision support system, and intelligent driving.

Jinghua Guo received the Ph.D. degree in vehicle dynamics control from the Dalian University of Technology, Dalian, China, in 2012.

From 2012 to 2015, he was a Post-Doctoral Research Fellow with Tsinghua University, Beijing, China. He is currently an Associate Professor with Xiamen University, Xiamen, China. He has authored over 30 journal papers. He has engaged over five sponsored projects. His current research interests include intelligent vehicles, vision system, control theory, and applications.

Hamid Taghavifar (M'18) received the Ph.D. degree in mechanical engineering from Urmia University, Urmia, Iran, in 2016.

He was a Vehicle Ride and Handling Engineer with Fiat Chrysler ARDC, Windsor, ON, USA and a Horizon Post-Doctoral Fellow with CONCAVE Research Center, Concordia University, Montreal, QC, Canada. He is currently an Assistant Professor with the School of Mechanical, Aerospace and Automotive Engineering, Coventry University, Coventry, U.K. He has contributed over 50 peer-reviewed papers, a book, and 2 Iranian registered patents. His current research interests include automated driving, control of autonomous systems (adaptive, nonlinear, and intelligent), robotics, and artificial intelligence.

Dr. Taghavifar serves as the Editor-in-Chief for the *Journal of Advances in Vehicle Engineering* and a Editor for the *International Journal of Vehicle Systems Modelling and Testing* and the *International Journal of Vehicle Information and Communication Systems*.

Yechen Qin (S'12–M'16) received the B.Sc. and Ph.D. degrees in mechanical engineering from the Beijing Institute of Technology, Beijing, China, in 2010 and 2016, respectively.

He is currently an Associate Professor with the Beijing Institute of Technology. From 2013 to 2014, he was a visiting Ph.D. student with Texas A&M University, College Station, TX, USA. He was also a Post-Doctoral Research Fellow and a Visiting Scholar with the Beijing Institute of Technology and University of Waterloo, Waterloo, ON, Canada. His current research interests include vehicle dynamics control and road estimation.

Jing Na (M'15) received the B.Eng. and Ph.D. degrees in control engineering from the School of Automation, Beijing Institute of Technology, Beijing, China, in 2004 and 2010, respectively.

From 2011 to 2013, he was a Monaco/ITER Post-Doctoral Fellow with ITER Organization, Saint-Paul-lès-Durance, France. From 2015 to 2017, he was a Marie Curie Intra-European Fellow with the Department of Mechanical Engineering, University of Bristol, Bristol, U.K. Since 2010, he has been with the Faculty of Mechanical and Electrical Engineering, Kunming University of Science and Technology, Kunming, China, where he became a Full Professor in 2013. He has coauthored one monograph published in Elsevier and authored or coauthored over 100 international journals and conference papers. His current research interests include intelligent control, adaptive parameter estimation, nonlinear control and applications for robotics, vehicle systems, and wave energy convertor.

Dr. Na was a recipient of the Marie Curie Fellowship from EU, the Best Application Paper Award of the 3rd IFAC International Conference on Intelligent Control and Automation Science in 2013, and the 2017 Hsue-Shen Tsien Paper Award. He is currently an Associate Editor of *Neurocomputing* and has served as the IPC Chair for ICMIC in 2017.

Chongfeng Wei received the B.Sc. degree in computational and applied mathematics and the M.Sc. degree in vehicle engineering from Southwest Jiaotong University, Chengdu, China, in 2009 and 2011, respectively, and the Ph.D. degree in mechanical engineering from the University of Birmingham, Birmingham, U.K., in 2015.

He joined the School of Mechanical Engineering, Shanghai Jiao Tong University, Shanghai, China, as an Assistant Professor (tenure-track). He then moved to the Institute of Transport Studies, University of Leeds, Leeds, U.K., as a Research Fellow in 2018. His current research interests include human-like autonomous vehicle control and collision avoidance.